Effects of the electron energy distribution on the plasma chemistry in argon: A time dependent global (volume averaged) model study

by

Einar Guðfinnsson and Jón Tómas Guðmundsson

RH-22-2000

Science Institute

University of Iceland

Effects of the electron energy distribution on the plasma chemistry in argon: A time dependent global (volume averaged) model study

E. Gudfinnsson and J. T. Gudmundsson

Science Institute, University of Iceland, Dunhaga 3, IS-107 Reykjavík, Iceland

(17th October 2000)

Abstract

We study the effect of varying the electron energy distribution, from being Maxwellian to Druyvesteyn like, on the plasma parameters of argon discharge by a time dependent global (volume averaged) model. We find the electron density to decrease and the effective electron temperature and the metastable argon density to increase as the electron energy distribution is varied from being Maxwellian like to Druyveseyn like. The ratio of the sheath voltage V_s to the effective electron energy T_{eff} decreases as the electron energy distribution function is varied from being Maxwellian to become Druyvesteyn like. Furthermore, we investigated the effect of varying the electron energy distribution on the plasma parameters of a pulsed discharge. The average electron density is higher for a pulsed discharge than for a continuous one for the same average power. As the electron energy distribution is varied in a pulsed discharge the ratio of the average electron density in a pulsed discharge to the electron density in a continous wave discharge at the same average power changes slightly, it decreases for 1 ms period, remains roughly constant for 100 μs period and increases for 10 μs period.

I. INTRODUCTION

The effect of the electron energy distribution on the plasma parameters is of practical interest in a high density low pressured discharge. Lieberman and Gottscho [1] proposed a simple global model of argon-plasma by assuming steady state and neglecting excited atoms. This global model was extended to include molecules [2] and mixtures [2,3]. The main idea of a global model is to neglect the complexity which arises when spatial variations are considered and to generate a model that encompasses large number of reactions in order to model a processing plasma with a limited computing power. Usually the reaction rate coefficients for electron collisions are calculated by integrating the collision cross sections over a Maxwellian electron energy distribution [1,2]. The Maxwell electron energy distribution applies to an assembly of particles in complete thermal equilibrium whereas the electrons in a glow discharge are in a non-equilibrium state. The slower electrons experience only elastic collisions while electrons with energies above excitation and ionization thresholds can loose a fraction of their energy through inelastic processes. Furthermore, fast electrons are lost rapidly by diffusion to walls. Thus, we expect to have a depletion in the electron energy distribution at high energies [4]. Druyvesteyn and Penning [5] considered the motion of electrons in a weak electric field but ignoring inelastic collisions. The resulting electron energy distribution is known as Druyvesteyn distribution. The Druyvesteyn distribution predicts more electrons with energies around the average energy and fewer electrons at higher energy than does Maxwell distribution. In the more elaborate global model of argon discharge, Lee *et al* [2] included metastable Ar^*, while other excited argon-states were neglected. In a time dependent global model, Ashida *et al* [6] considered the two main groups of excited states, $Ar(4s)$ and $Ar(4p)$, neglecting others. Excitation cross section from a ground state atoms to every four of the $Ar(4s)$-states were published by Tachibana [7], and Eggarter published the excitation cross section of other excited states [8]. In this work we will investigate how varying the electric energy distribution function from Maxwellian like to being Druyvesteyn like affects the time dependent behavior of plasma parameters such as electron density, effective electron temperature, sheath potential and the density of metastable argon atoms. It should be emphasized that the global model is not accurate. It is limited by the fact that it is volume averaged and the accuracy of the cross section data.

II. THE GLOBAL (VOLUME AVERAGED) MODEL

A. Sheath edge density

The ratios of the density at the sheath edge to that in the bulk for the axial and radial directions, denoted by h_{L} and h_{R} respectively, and are derived from low pressure diffusion theory, $(R, L) \leq \lambda_{\mathrm{i}} \leq (T_{\mathrm{i}}/T_{\mathrm{e}})(R, L)$, by [9,10]

$$h_{\mathrm{L}} = 0.86\left[3 + \frac{L}{2\lambda_{\mathrm{i}}}\right]^{-\frac{1}{2}} \tag{1}$$

$$h_{\mathrm{R}} = 0.8\left[4 + \frac{R}{\lambda_{\mathrm{i}}}\right]^{-\frac{1}{2}}, \tag{2}$$

where λ_{i} is the ion-neutral mean free path. The ratios h_{L} and h_{R} depend only on the ion mean free path (the operating pressure) and the dimensions of the discharge. The dominating cross sections for the ion-neutral collision in argon are resonant charge transfer and elastic scattering. The combined ionic momentum transfer cross section for these two processes is roughly 1×10^{-18} m^2 for the thermal energies of interest [11]. In our model we assume that $R = 15.24\,\mathrm{cm}$ and $L = 7.6\,\mathrm{cm}$. Another critical value is the gas temperature, which is usually given rather arbitrary by authors. We assume $T_{\mathrm{g}} = 473$ K.

B. Electron collisional energy loss per electron-ion

One of the most vital quantity for finding the electron density using the global model is the electron collisional energy loss per electron-ion pair created by ionization, $\mathcal{E}_{\mathrm{c}}$. $\mathcal{E}_{\mathrm{c}}$ depends highly on the rate of excitations and is given by

$$\mathcal{E}_{\mathrm{c}} = \mathcal{E}_{\mathrm{iz}} + \sum_i \mathcal{E}_{\mathrm{ex,i}} \frac{k_{\mathrm{ex,i}}}{k_{\mathrm{iz}}} + \frac{k_{\mathrm{el}}}{k_{\mathrm{iz}}} \frac{3m_{\mathrm{e}}}{m_{\mathrm{i}}} T_{\mathrm{eff}}, \tag{3}$$

where $\mathcal{E}_{\mathrm{iz}}$ is the ionization energy, $\mathcal{E}_{\mathrm{ex,i}}$ is the energy for the i-th excitation process, k_{iz} is the ionization rate constant, $k_{\mathrm{ex,i}}$ is the rate constant for the i-th excited state and k_{el} is the elastic scattering rateconstant. The effective electron temperature T_{eff} is defined as $T_{\mathrm{eff}} = \frac{2}{3}\langle\mathcal{E}\rangle$ where $\langle\mathcal{E}\rangle$ is the average electron energy.

The excitation rate constants are estimated by integrating measured excitation cross sections over the electron energy distribution. Tachibana [7] was first to measure the cross section for excitation to the $1s_5, 1s_4, 1s_3$, and $1s_2$ levels of the argon atom. His values for the $1s_5, 1s_3$ metastable states are considerably lower than was commonly accepted for the $4s$ states [12]. Resent measurements [13–17] are in agreement with the measurement of Tachibana. Thus we use Tachibana's cross-section in our model. Even though all

excitation cross-sections are needed to find the electron density, the lifetime of many of the excited states is small enough to be neglected. The most vital cross sections are those of the metastable states, since their life-time is relatively long compared to others excited states with similar excitation rate-constant. The resonance levels, $1s_2$ and $1s_4$ have a much shorter life-time than the metastable once, because of a high emission rate of the argon-resonance.

C. The differential equations for particle balance

The general equations used to describe the system are given by

$$\begin{aligned} \frac{dn_{\mathrm{Ar}^*}}{dt} &= \sum_i k_{\mathrm{col}} n_j n_k - \frac{D_{\mathrm{eff}}}{\Lambda^2} n_{\mathrm{Ar}^*} \\ \frac{dn_{\mathrm{e}}}{dt} &= \sum_i k_{\mathrm{iz,i}} n_{\mathrm{e}} n_i - k_{\mathrm{loss}} n_{\mathrm{e}} \end{aligned} \tag{4}$$

along with equation (3) for $\mathcal{E}_{\mathrm{c}}$.

The reactions we assumed in our model are listed in table I. Thus the general differential equations describing the particle balance become

$$\begin{aligned} \frac{dn_{\mathrm{Ar}^*}}{dt} &= k_{\mathrm{exc}} n_{\mathrm{e}} n_{\mathrm{g}} - k_{\mathrm{exc,iz}} n_{\mathrm{e}} n_{\mathrm{Ar}^*} - k_{\mathrm{rad}} n_{\mathrm{e}} n_{\mathrm{Ar}^*} - k_{\mathrm{exc,wall}} n_{\mathrm{Ar}^*} \\ \frac{dn_{\mathrm{e}}}{dt} &= k_{\mathrm{iz}} n_{\mathrm{e}} n_{\mathrm{g}} + k_{\mathrm{exc,iz}} n_{\mathrm{e}} n_{\mathrm{Ar}^*} - k_{\mathrm{wall}} n_{\mathrm{e}}. \end{aligned} \tag{5}$$

Furthermore, we define the neutral argon density, n_{g} as

$$n_{\mathrm{g}} = n_{\mathrm{Ar}} + \sum n_{\mathrm{Ar}_{\mathrm{exc}}} = p_{\mathrm{g}} T_{\mathrm{g}} k_{\mathrm{B}} \tag{6}$$

where p_{g} is the gas pressure and k_{B} is the Boltzmann constant. We assume $n_{\mathrm{Ar}} = n_{\mathrm{g}}$.

III. THE ELECTRON ENERGY DISTRIBUTION FUNCTION (EEDF)

When altering the electron energy distribution function from Maxwellian like to Druyvesteyn like, the rate constants become more dependent on the cross-section at low energy ($\lesssim$ 20 V). The variation in $\mathcal{E}_{\mathrm{c}}$ as a function of the effective electron temperature T_{eff} can be seen in figure 1. If the velocity space is isotropic a general equation for the electron energy distribution function can be expressed as [18]

$$f(\mathcal{E}) = c_1 \mathcal{E}^{1/2} \exp\left(-c_2 \mathcal{E}^x\right) \tag{7}$$

where $\mathcal{E}$ is the electron energy, and c_1 and c_2 are constants that depend on the electron energy distribution. Here $x = 1$ and $x = 2$ correspond to Maxwellian and Druyvesteyn

electron energy distribution representing elastic collision cross sections that are inversely proportional to and independent of the electron velocity, respectively. The constants c_1 and c_2 are given by [19]

$$c_1 = \frac{x}{\langle \mathcal{E} \rangle^{\frac{3}{2}}} \frac{[\Gamma(\xi_2)]^{3/2}}{[\Gamma(\xi_1)]^{5/2}} \tag{8}$$

and

$$c_2 = \frac{1}{\langle \mathcal{E} \rangle^x} \left[\frac{\Gamma(\xi_2)}{\Gamma(\xi_1)} \right]^x . \tag{9}$$

Figure 2 shows the electron energy probability function (EEPF) defined as $\mathcal{E}^{-1/2} f(\mathcal{E})$ versus electron energy for $T_{\text{eff}} = 3$ eV and $x = 1.0, 1.25, 1.5$ and 2.0. We note that the number of fast electrons is highest for the Maxwellian distribution and decreases as we approach Druyvesteyn distribution [5].

A. Other parameters

To find the general equation for the ion- and electron velocity and the average kinetic energy lost per ion and electron lost we follow [19]. A general equation for the ion velocity is given by

$$v_{\text{i}} = \langle \mathcal{E} \rangle^{1/2} \left(\frac{2}{m_{\text{i}}} \right)^{1/2} \frac{[\Gamma(\xi_1)]}{[\Gamma(\xi_2)\Gamma(\xi_3)]^{1/2}} \tag{10}$$

This leads to the Bohm criterion which for Maxwellian electron energy distribution is $u_{\text{B}} = (eT_{\text{e}}/m_{\text{i}})^{1/2}$.

For an arbitrary electron energy distribution the mean electron speed is given as

$$\bar{v}_{\text{e}} = \langle \mathcal{E} \rangle^{1/2} \left(\frac{2e}{m_{\text{e}}} \right)^{1/2} \frac{[\Gamma(\xi_4)]}{[\Gamma(\xi_1)\Gamma(\xi_2)]^{1/2}} \tag{11}$$

where $\xi_4 = 2/x$. For Maxwellian distribution the mean electron speed thus becomes $\bar{v}_{\text{e}} = (8eT_{\text{e}}/\pi m_{\text{e}})^{1/2}$.

The ion and electron fluxes at the discharge walls are $\Gamma_{\text{i}} = n_{\text{s}} v_{\text{i}}$ and $\Gamma_{\text{e}} = \frac{1}{4} n_{\text{s}} \bar{v}_{\text{e}} \delta_{\text{e}}$ where δ_{e} is the ratio of the electron density at the sheath edge to the electron density in the plasma bulk given by [20]

$$\delta_{\text{e}} = \int_{eV_{\text{s}}}^{\infty} \sqrt{1 - \frac{eV_{\text{s}}}{\mathcal{E}}} f(\mathcal{E}) d\mathcal{E} \tag{12}$$

where $f(E)$ is the electron energy distribution function. For an insulating wall, the ion and electron fluxes must balance in steady state which gives a criterium to find the sheath voltage, namely by the equation

$$\frac{4v_{\rm i}}{\overline{v}_{\rm e}} = \int_{eV_{\rm s}}^{\infty} \sqrt{1 - \frac{eV_{\rm s}}{\mathcal{E}}} f(\mathcal{E}) d\mathcal{E}. \tag{13}$$

For Maxwellian distribution the sheath voltage is thus given by

$$V_{\rm s} = T_{\rm eff} \ln \left(\frac{\bar{v}_{\rm e}}{4v_{\rm i}} \right), \tag{14}$$

or $V_{\rm s} \approx 4.7 T_{\rm e}$. For the general electron energy distribution, we calculated $V_{\rm s}$ numerically, and found that $V_s \propto T_{\rm eff}$ for $T_{\rm eff} < 15$ eV. The results are shown in figure 3 where the ratio of the sheath potential $V_{\rm s}$ to the effective electron temperature $T_{\rm eff}$ is shown as a function of the parameter x.

The mean kinetic energy lost per electron lost is calculated as the ratio of the average energy flux $S_{\rm e}$ to the electron flux $\Gamma_{\rm e}$ [21]. For the general electron energy distribution given by equation (7) the average kinetic energy per electron lost is given by

$$\mathcal{E}_{\rm e} = \left(\frac{\Gamma(\xi_1)\Gamma(\xi_5)}{\Gamma(\xi_2)\Gamma(\xi_4)} \right) \langle \mathcal{E} \rangle \tag{15}$$

where $\xi_5 = 3/x$. For Maxwellian electron energy distribution the mean electron energy lost per electron lost is thus $\mathcal{E}_{\rm e} = 2T_{\rm e}$.

The mean kinetic energy lost per ion lost is the sum of the ion energy entering the sheath and the energy gained by the ion as it traverses the sheath

$$\mathcal{E}_{\rm i} = \langle \mathcal{E} \rangle \frac{[\Gamma(\xi_1)]^2}{[\Gamma(\xi_2)\Gamma(\xi_3)]} + V_{\rm s} \tag{16}$$

For Maxwellian electron energy distribution and argon ions $\mathcal{E}_{\rm i} \approx 5.2 T_{\rm e}$.

IV. STEADY STATE

The ratio of the sheath voltage $V_{\rm s}$ to the effective electron temperature $T_{\rm eff}$ is shown in figure 3. The ratio decreases as the electron energy distribution is varied from Maxwellian to to become Druyvesteyn like. We find $V_{\rm s} \approx 4.7 T_{\rm eff}$ for $x = 1$, $V_{\rm s} \approx 4.2 T_{\rm eff}$ for $x = 1.25$, $V_{\rm s} \approx 3.8 T_{\rm eff}$ for $x = 1.5$ and $V_{\rm s} \approx 3.4 T_{\rm eff}$ for $x = 2$. Separate calculations have shown that the sheath voltage decreases as the electron energy distribution function is varied from being Maxwellian to become Druyvesteyn like for low pressures (< 2 mTorr) and increases for higher pressures as the electron energy distribution function is varied [19].

We use our formulation above to calculate the electron density in a steady state for several values of applied power and pressure, for $x = 1$ and $x = 2$. The results are shown in figures 4 and 5. The center electron density is shown as a function of the pressure in figures 4 for Maxwellian electron energy distribution and in figure 5 for Druyvesteyn electron energy distribution for various discharge power values $P_{\rm abs}$. The electron density decreases as the electron energy distribution function is varied by a factor 1.5 at 1 mTorr and 2.5 at 20 mTorr and $P_{\rm abs} = 500$ W. The effective electron temperature in steady state is practically independent of power. Thus we show the effective electron temperature as a function of pressure for Maxwellian electron energy distribution and Druyvesteyn distribution in figure 6. The effective electron temperature is a factor 1.3 higher for Druyvesteyn distribution than for Maxwellian distribution at 1 mTorr and a factor 1.8 higher at 50 mTorr. The metastable argon atom density, $n_{\rm Ar^*}$ increases as the applied power is increased. We show how $n_{\rm Ar^*}$ varies with pressure for Maxwellian and Druyvesteyn distribution respectively in figure 7. We note that the metastable argon density increases by a factor of 1.5 at 1 mTorr and a factor of 2.8 at 50 mTorr as the electron energy distribution is varied from being Maxwellian like to being Druyvesteyn like. Furthermore, we calculated the electron density $n_{\rm e}$ by the time-independent model, which neglects excited atoms and compare it to calculation which include the excited states. The results are shown in figure 8 which shows the ratio of the electron density calculated by time dependent model including metastables to the electron energy density calculated by the simple time-independent model that neglects metastable states. The electron density is roughly 0.5 % higher at 1 mTorr and 4 % higher at 50 mTorr if the metastable states are included.

V. PULSED DISCHARGE

Using the global model to study pulsed power induces some problems. The electron temperature approaches zero as the power is turned off. When the electron temperature is low, all calculations become very sensitive, as $\mathcal{E}_{\rm c}$ goes to infinity and all the rateconstants tend to zero. In many cases the rate-constants are given as constants, independent of the electron temperature, which may be an inappropriate approximation if the electron temperature is low. This introduced some difficulty when calculating the behavior of $p_{\rm e}$ as a function of time, for long periods. Due to instability in the calculations, $p_{\rm e}$ could go a little below zero, when the power had been set to zero for some time. We therefore changed the program, forcing $p_{\rm e}$ to be positive at all times. Due to this the electron temperature is inaccurate when the power has been turned off for some time. This has

the effect that when the power is turned on again, the jump which occurs in the effective electron temperature is not expected to be accurate. On the other hand the relaxation time can be assumed to be reasonable.

We assume that the power is modulated by ideal rectangular waves. Two waves are considered, for different periods. The waves have the same average power of 500 W, and are given by:

$$P_{\rm abs}(t) = P_{2000}(t) := \begin{cases} 2000\,{\rm W}, & 0 < t < \alpha\tau \\ 0\,{\rm W}, & \alpha\tau < t < \tau \end{cases} \tag{17}$$

and

$$P_{\rm abs}(t) = P_{1700}(t) := \begin{cases} 1700\,{\rm W}, & 0 < t < \alpha\tau \\ 100\,{\rm W}, & \alpha\tau < t < \tau \end{cases} \tag{18}$$

where $\alpha = 0.25$ is the duty ratio, and τ is the period. The results are shown in figures 9-14 for one period. Furthermore, we also calculated the average electron density, and compared it to the average electron density obtained when constant 500 W power is applied.

In figures 9-14 we see the center electron density $n_{\rm e}$, effective electron temperature $T_{\rm eff}$ and the metastable argon density for a pulsed discharge for $x = 1.0, 1.25, 1.5$ and 2.0. In the figures the period is varied from $\tau = 1$ ms in figure 9, $\tau = 100\,\mu$s in figure 10 to $\tau = 10\,\mu$s in figure 11 for $P_{\rm abs} = P_{2000}$ while the duty ratio is kept fixed at $\alpha = 0.25$ and the average power is 500 W. Similarly the period is varied from $\tau = 1$ ms in figure 12, $\tau = 100\,\mu$s in figure 13 to $\tau = 10\,\mu$s in figure 14 for $P_{\rm abs} = P_{1700}$ while the duty ratio is kept fixed at $\alpha = 0.25$ and the average power is 500 W. For $\tau = 100\,\mu$s the average electron density is more than twice as high as at $\tau = 1$ ms. In figures 9-14 the horizontal lines show corresponding values for continous wave at the same average power.

In figure 15 we see the ratio of the average electron density for $P_{\rm abs} = P_{1700}$ W to average electron density for $P_{\rm abs} = 500$ W (cw) versus the parameter x. In both cases the average applied power is 500 W. We note that the average electron density is higher for pulsed discharge than for a continuous wave. This consistent with the findings of Ashida *et al* [6] which were later confirmed by experiments [22]. The average electron density increases slightly for 10 μs period but decreases slightly for 1 ms period when the electron energy distribution is varied from being Maxwellian like to being Druyvesteyn like. Similar findings are shown in figure 16 where the ratio of the average electron density for $P_{\rm abs} = P_{2000}$ W to average electron density for $P_{\rm abs} = 500$ W (cw) is shown versus the parameter x.

VI. CONCLUSION

We developed a time dependent global (volume averaged) model of an argon discharge to investigate the effect of varying the electron energy distribution on the plasma parameters in the discharge.

The electron density decreases, the effective electron temperature and the metastable argon density increases as the electron energy distribution function is varied from being Maxwellian to become Druyvesteyn like in steady state. The ratio of the sheath voltage V_s to the effective electron energy T_{eff} decreases as the electron energy distribution function is varied from being Maxwellian to become Druyvesteyn like. The ratio of the average electron density is higher for pulsed discharge than for a continous one. As the electron energy distribution is varied in a pulsed discharge the ratio of the average electron density to the electron density for a continous wave at the same average power changes slightly, it decreases for 1 ms period, remains roughly constant for 100 μs period and increases for 10 μs period.

It should be emphasized that the global model is not meant to give accurate values of the plasma parameters but it can give an indication how one parameter depends on another.

ACKNOWLEDGMENTS

This work was partially supported by the Icelandic Student Innovation Fund, Icelandic Research Council and the University of Iceland Research Fund.

References

[1] M. A. Lieberman and R. A. Gottscho, in *Physics of Thin Films, vol. 18*, edited by M. Francombe and J. Vossen (Academic Press, New York, 1994), pp. 1 – 119.

[2] C. Lee and M. A. Lieberman, Journal of Vacuum Science and Technology A **13**, 368 (1995).

[3] K. K. Patel, Master's thesis, University of California at Berkeley, 1998.

[4] B. Chapman, *Glow Discharges Processes* (John Wiley & Sons, New York, 1980).

[5] M. J. Druyvesteyn and F. M. Penning, Reviews of Modern Physics **12**, 87 (1940).

[6] S. Ashida, C. Lee, and M. A. Lieberman, Journal of Vacuum Science and Technology A **13**, 2498 (1995).

[7] K. Tachibana, Physical Review A **34**, 1007 (1986).

[8] E. Eggarter, Journal of Chemical Physics **62**, 833 (1975).

[9] V. A. Godyak and V. N. Maximov, Vestnik Moskovskogo Universiteta, ser. Physica i Astronomia **18**, 51 (1977).

[10] V. A. Godyak, *Soviet Radio Frequency Discharge Research* (Delphic Associates, Falls Churc V.A., 1986).

[11] M. A. Lieberman and A. J. Lichtenberg, *Principles of Plasma Discharges and Materials Processing* (John Wiley & Sons, New York, 1994), p. 80.

[12] W. L. Borst, Physical Review A **9**, 1195 (1974).

[13] J. E. Chilton, J. B. Boffard, R. S. Schappe, and C. C. Lin, Physical Review A **57**, 267 (1998).

[14] S. Tsurubuchi, T. Miyazaki, and K. Motohashi, Journal of Physics B: Atomic, Molecular and Optical Physics **29**, 1785 (1996).

[15] A. Dasgupta, M. Blaha, and J. L. Guiliani, Physical Review A **61**, 012703 (1999).

[16] M. Tadokoro, H. Hirata, N. Nakano, Z. L. Petrovic, and T. Makabe, Physical Review E **58**, 7823 (1998).

[17] R. S. Schappe, M. B. Schulman, L. W. Anderson, and C. C. Lin, Physical Review A **50**, 444 (1994).

[18] H. Amemiya, Journal of the Physical Society of Japan **66**, 1335 (1997).

[19] J. T. Gudmundsson, Plasma Sources Science and Technology (Submitted).

[20] H. Amemiya, Journal of the Physical Society of Japan **67**, 1955 (1997).

[21] M. A. Lieberman and A. J. Lichtenberg, *Principles of Plasma Discharges and Materials Processing* (John Wiley & Sons, New York, 1994), p. 39.

[22] S. Ashida, M. R. Sim, and M. A. Lieberman, Journal of Vacuum Science and Technology A **14**, 391 (1996).

[23] H. C. Straub, P. Renault, B. G. Lindsay, K. A. Smith, and R. F. Stebbings, Physical Review A **52**, 1115 (1995).

TABLES

Table I. Reactions included in the model.

Reaction	Rateconstant	Cross section ref.
$\mathrm{Ar}+e \rightarrow \mathrm{Ar}^* + e$	k_{exc}	[7]
$\mathrm{Ar}+e \rightarrow \mathrm{Ar}^+ + 2e$	k_{iz}	[23]
$\mathrm{Ar}^* + e \rightarrow \mathrm{Ar}^+ + 2e$	$k_{\mathrm{exc,iz}}$	[2]
$\mathrm{Ar}^* \rightarrow \mathrm{Ar}+h\nu$	k_{rad}	[6]
$\mathrm{Ar}^+ \rightarrow \mathrm{Ar}$ (wall)	k_{wall}	[6]
$\mathrm{Ar}^* \rightarrow \mathrm{Ar}$ (wall)	$k_{\mathrm{exc,wall}}$	[6]

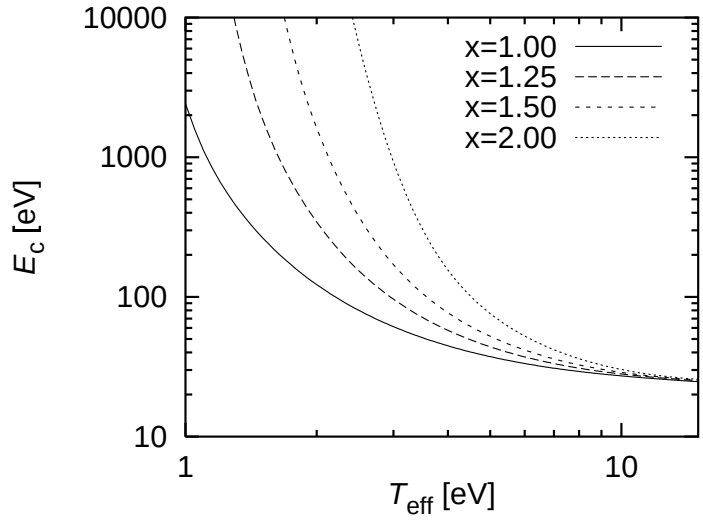

Figure 1. The electron collisional energy loss per electron-ion lost $\mathcal{E}_c$ as a function of the effective electron temperature T_{eff} for various values of the parameter x.

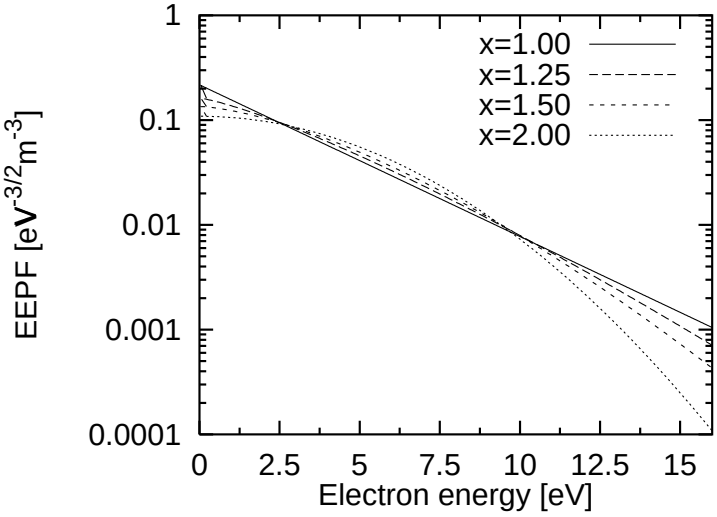

Figure 2. The electron energy probability function (EEPF) as a function of the electron energy for various values of the parameter x.

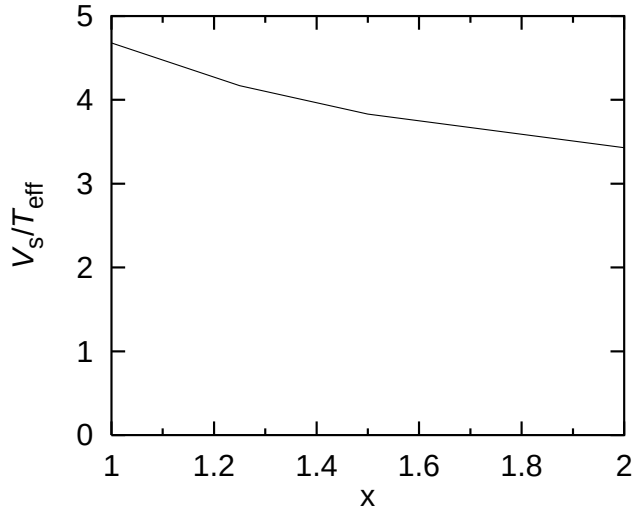

Figure 3. The ratio of the sheath potential to the effective electron temperature V_s/T_{eff} as a function of the parameter x.

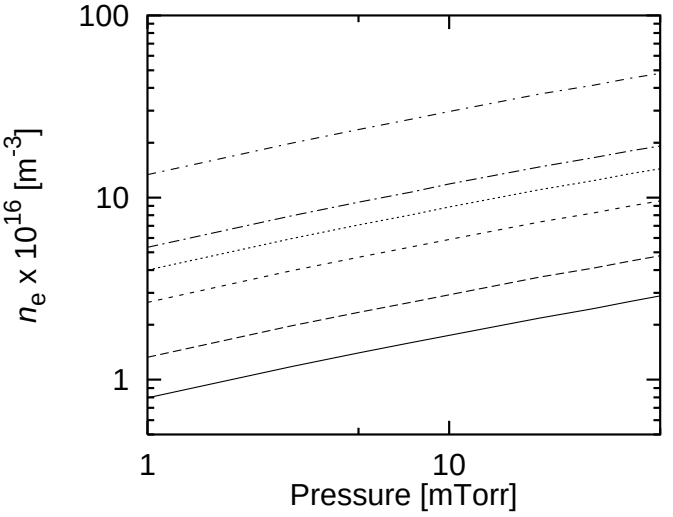

Figure 4. Electron density n_e in steady state as a function of pressure for applied power of 30 (lowest), 50, 100, 150, 200 and 500 (highest) W assuming Maxwellian electron energy distribution.

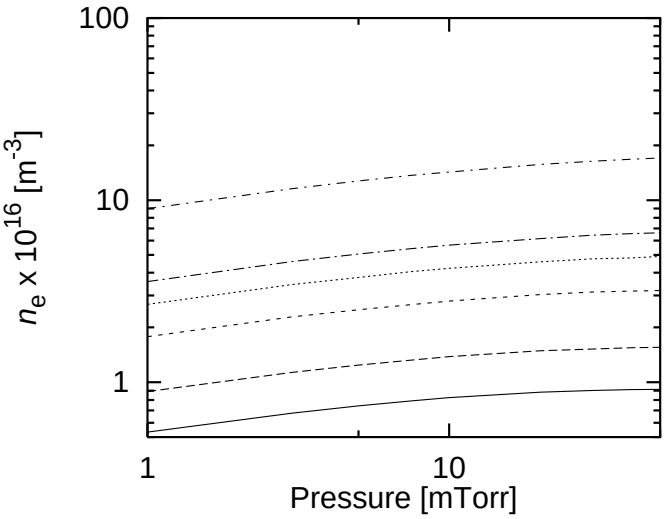

Figure 5. Electron density n_e in steady state as a function of pressure for applied power of 30 (lowest), 50, 100, 150, 200 and 500 (highest) W assuming Druyvesteyn electron energy distribution.

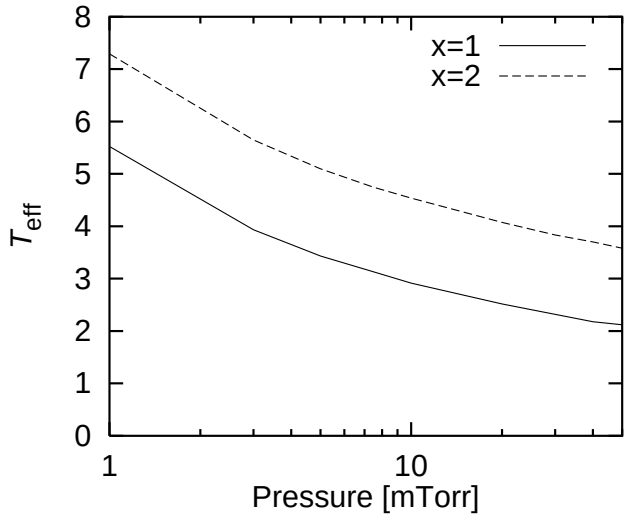

Figure 6. The effective electron temperature T_{eff} as a function of pressure after steady state has been reached assuming Maxwellian ($x = 1$) and Druyvesteyn ($x = 2$) electron energy distribution for $P_{\mathrm{abs}} = 500$ W.

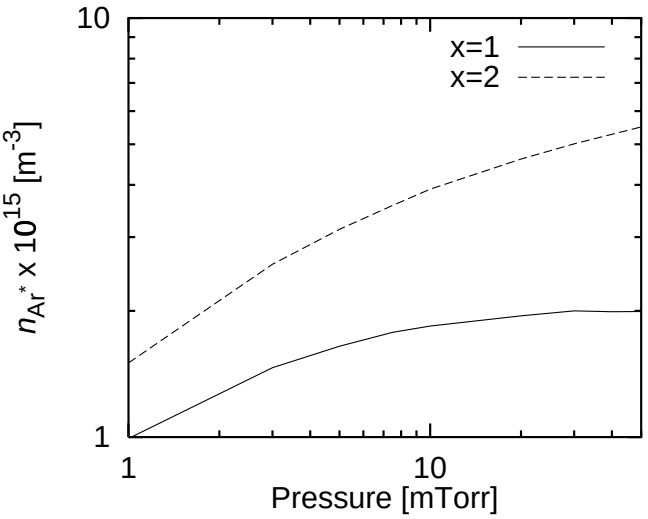

Figure 7. The argon metastable density n_{Ar^*} as a function of pressure after steady state has been reached assuming Maxwellian ($x = 1$) and Druyvesteyn ($x = 2$) electron energy distribution for $P_{\mathrm{abs}} = 500$ W.

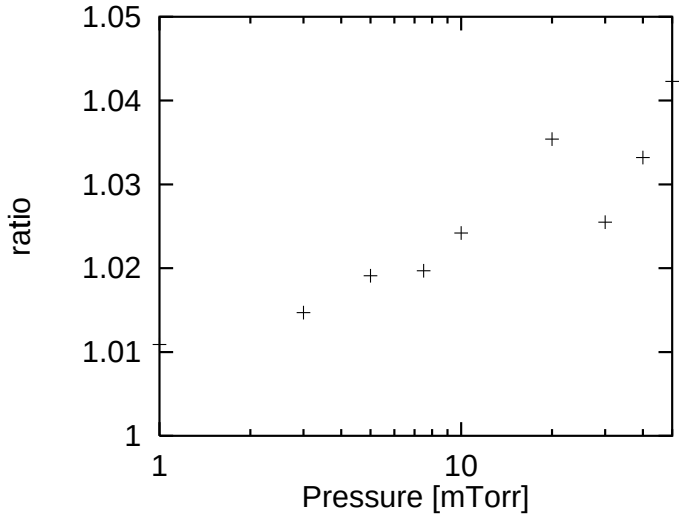

Figure 8. The ratio of the electron density after steady state has been reached assuming Maxwell electron energy distribution versus the electron density calculated by the simple time-independent model, which neglects excited states.

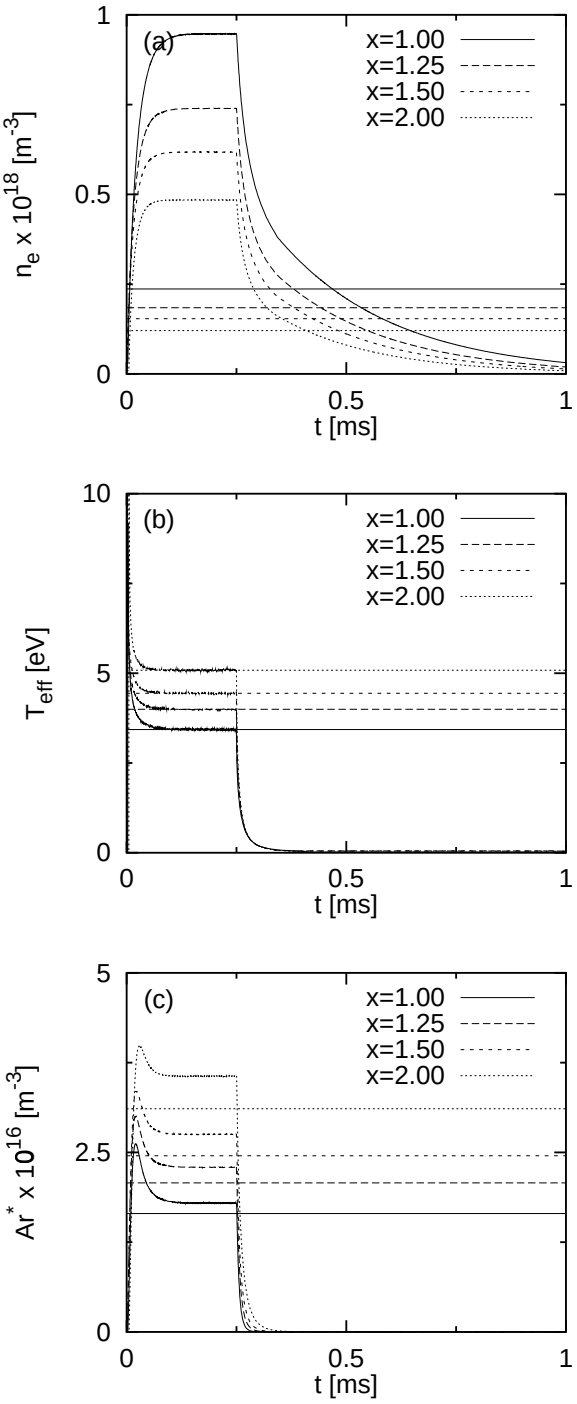

Figure 9. (a) The electron density n_e, (b) effective electron temperature T_{eff} and (c) the metastable argon density n_{Ar^*} for a pulsed argon discharge with $P_{\text{abs}} = P_{2000}$ W, $\tau = 1$ ms. The horizontal lines show the corresponding values for continous wave at the same averaged power 500 W.

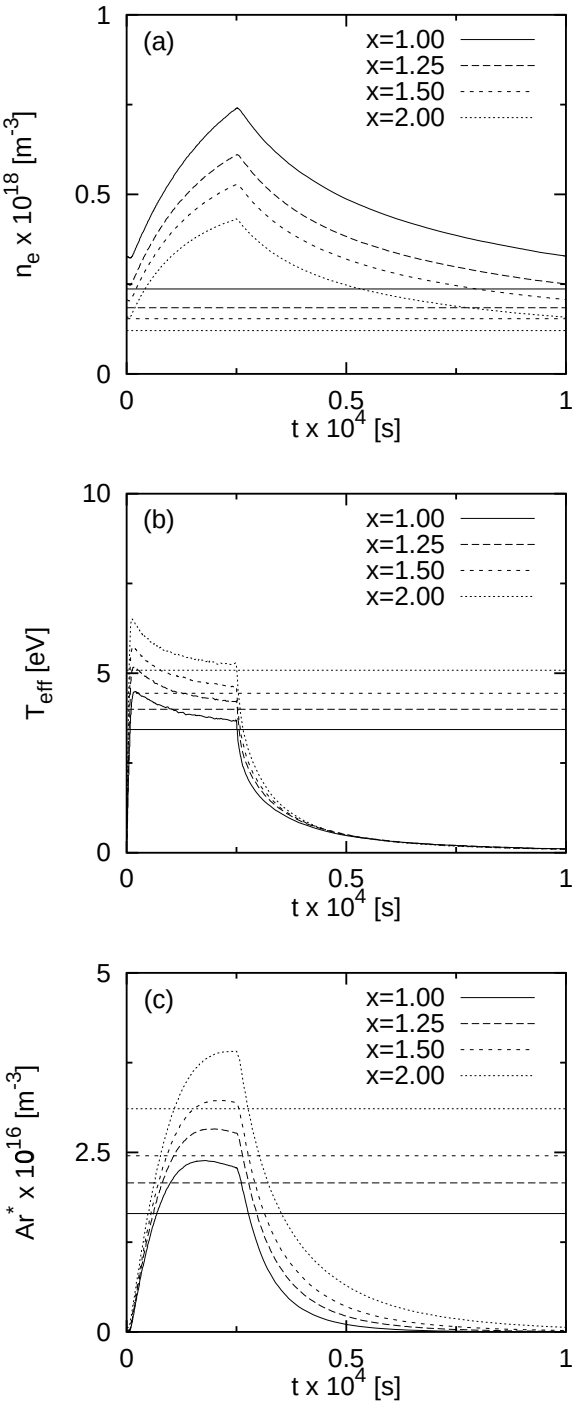

Figure 10. (a) The electron density n_e, (b) effective electron temperature $T_{\rm eff}$ and (c) the metastable argon density $n_{\rm Ar^*}$ for a pulsed argon discharge with $P_{\rm abs} = P_{2000}$ W, $\tau = 100$ μs. The horizontal lines show the corresponding values for continous wave at the same averaged power 500 W.

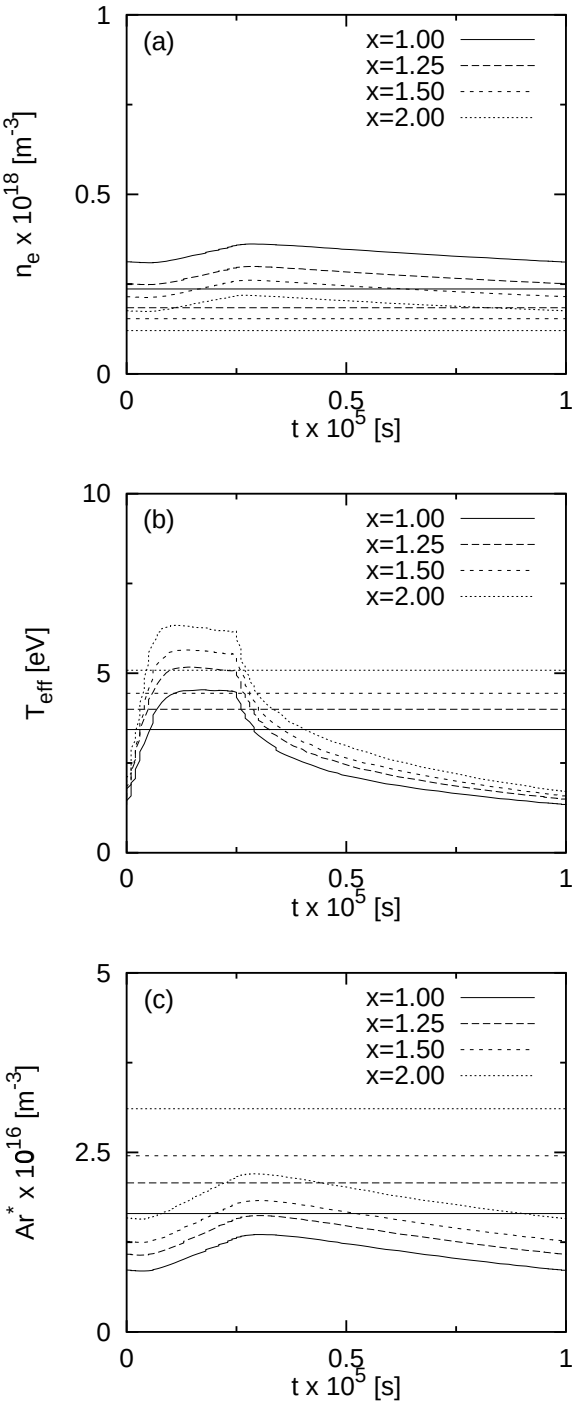

Figure 11. (a) The electron density n_e, (b) effective electron temperature $T_{\rm eff}$ and (c) the metastable argon density $n_{\rm Ar^*}$ for a pulsed argon discharge with $P_{\rm abs} = P_{2000}$ W, $\tau = 10$ μs. The horizontal lines show the corresponding values for continous wave at the same averaged power 500 W.

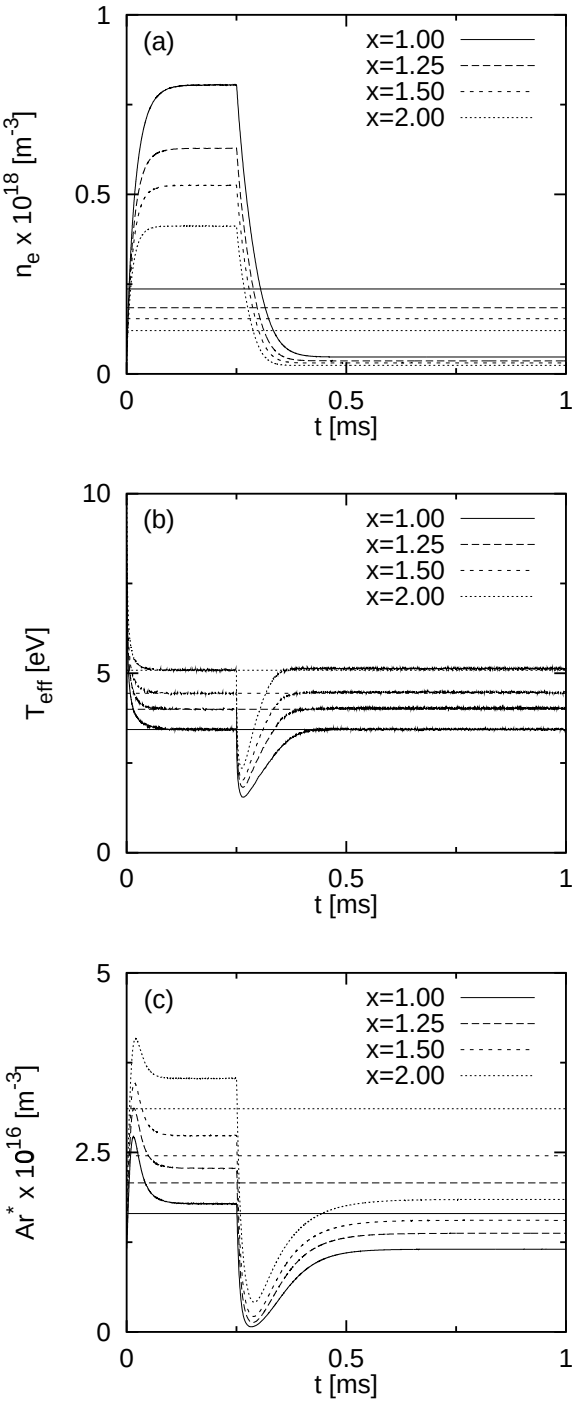

Figure 12. (a) The electron density n_e, (b) effective electron temperature T_{eff} and (c) the metastable argon density n_{Ar^*} for a pulsed argon discharge with $P_{\text{abs}} = P_{1700}$ W, $\tau = 1$ ms. The horizontal lines show the corresponding values for continous wave at the same averaged power 500 W.

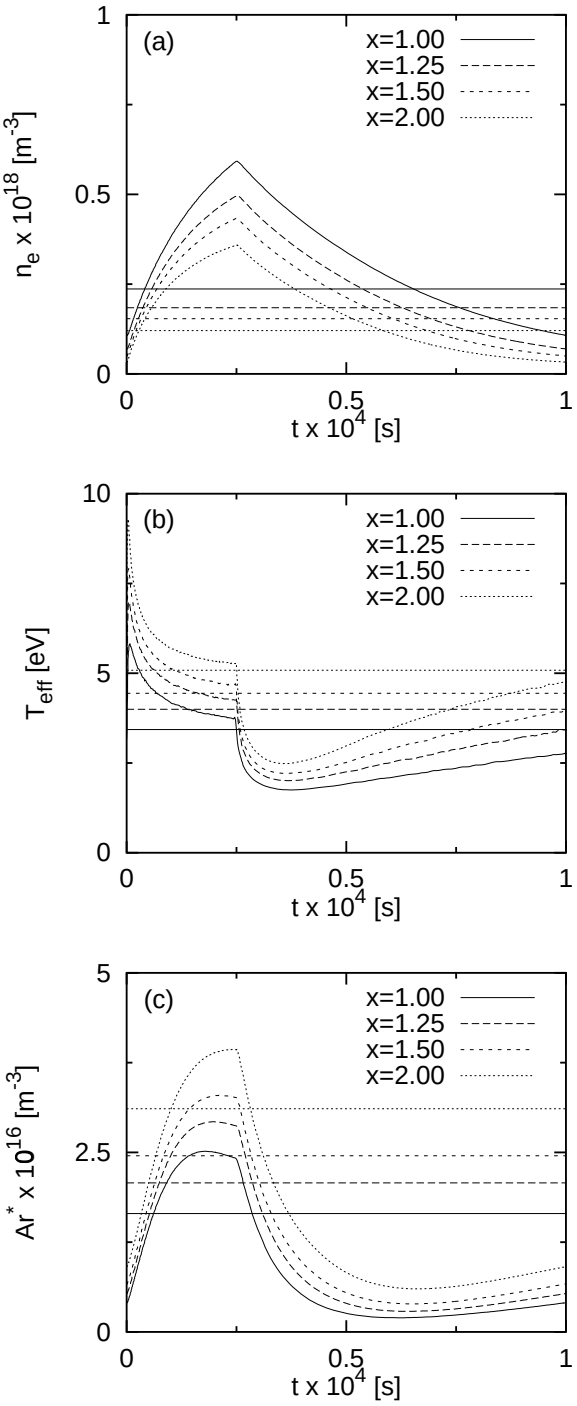

Figure 13. (a) The electron density n_e, (b) effective electron temperature $T_{\rm eff}$ and (c) the metastable argon density $n_{\rm Ar^*}$ for a pulsed argon discharge with $P_{\rm abs} = P_{1700}$ W, $\tau = 100$ μs. The horizontal lines show the corresponding values for continous wave at the same averaged power 500 W.

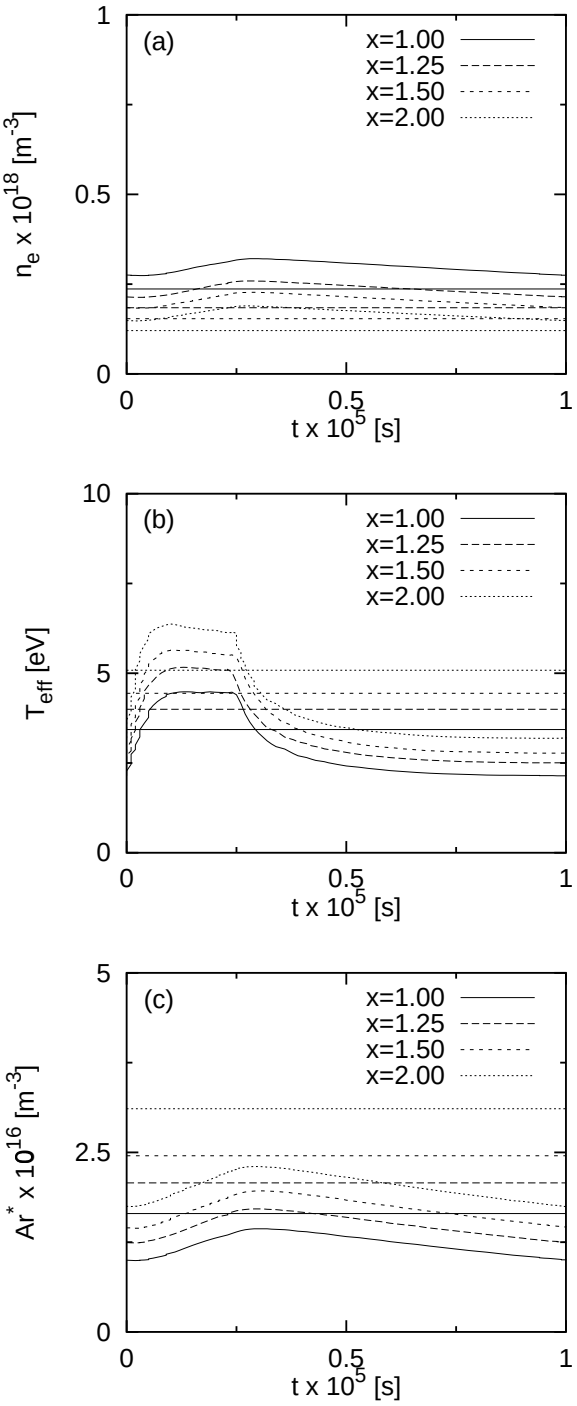

Figure 14. (a) The electron density n_{e}, (b) effective electron temperature T_{eff} and (c) the metastable argon density n_{Ar^*} for a pulsed argon discharge with $P_{\mathrm{abs}} = P_{1700}$ W, $\tau = 10$ μs. The horizontal lines show the corresponding values for continous wave at the same averaged power 500 W.

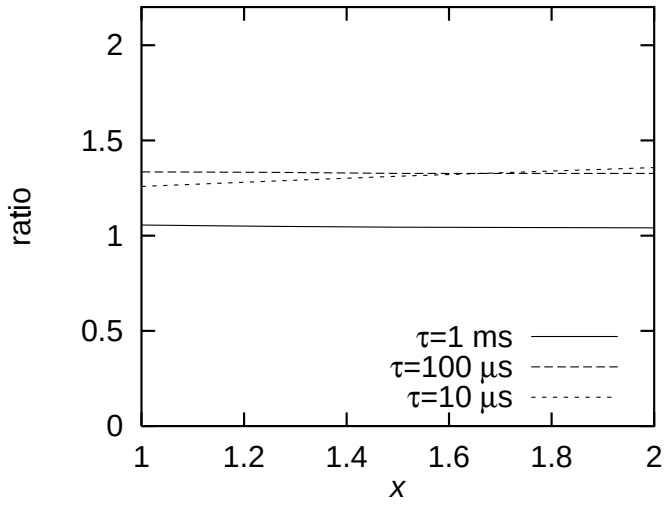

Figure 15. The ratio of the average electron densitiy for $P_{\mathrm{abs}} = P_{1700}$ W to average electron density for $P_{\mathrm{abs}} = 500$ W (cw) versus the parameter x.

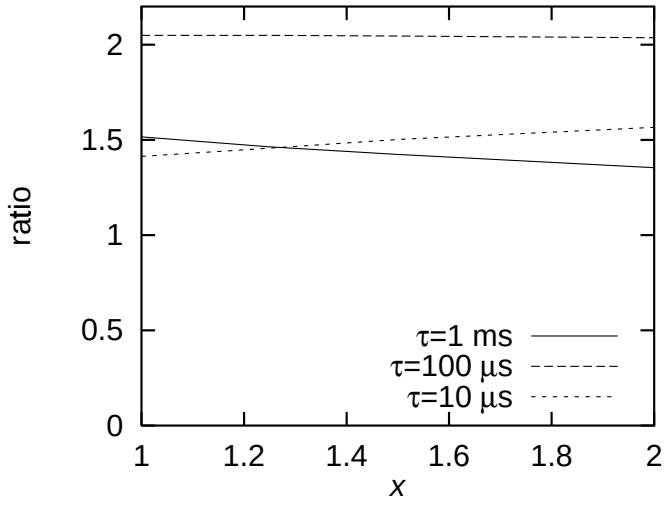

Figure 16. The ratio of the average electron densitiy for $P_{\mathrm{abs}} = P_{2000}$ W to average electron density for $P_{\mathrm{abs}} = 500$ W (cw) versus the parameter x.